Diagnosing Quality Problems on a Complex CNC Machine via Process-oriented Basis Representations

Burak Birgören

Industrial Engineering Department, Kirikkale University, Kirikkale, 71451 Turkey.
Phone: +90 (318) 357-4242 / 1006; Fax: +90 (318) 357-2459, birgoren@kku.edu.tr

Abstract— A Process-oriented basis representation (POBREP) can be used to express a multivariate quality vector as a linear combination of fault patterns, plus a residual. Monitoring the estimated coefficients of the linear relationship is especially useful when the quality vector contains the same kind of measurements at different locations on a product. Such an application is the subject of this study. POBREPs are derived for different types of quality problems for a 9-axis CNC drilling machine; complicated geometry involved in the drilling operation makes the derivation process a challenging task. Therefore a thorough treatment of the derivation process is presented. Next, diagnostic power of the POBREP is demonstrated by an application to multivariate process data.

Index Terms—**Multivariate Quality Control, Process-oriented**

I. INTRODUCTION

The process-oriented basis representation (POBREP) is a process diagnostic methodology for identifying likely causes of quality problems by decomposing multivariate quality data into cause-associated components. It is particularly applicable when the quality measurements are taken from multiple locations of a product, e.g. thickness, diameter, resistivity, etc. This methodology was first described by Barton and González-Barreto [1] and was further studied and enhanced by Birgoren [2, 3]. An application to electronics manufacturing was also provided by Colon and González-Barreto [4]. This study examines a POBREP application discussed previously by Birgoren [2] to highlight modeling and application issues for diagnosing quality problems in CNC machining via the POBREP methodology.

The POBREP methodology has been studied for multivariate Statistical Process Control (SPC) by several authors in recent years [5, 6]. The main reason for this interest is lack of process-driven techniques in the multivariate SPC literature. Traditionally, multivariate SPC techniques have been data-driven, that is, they do not use any priori knowledge that might help understand and interpret quality problems observed in the data. Lowry and Montgomery [7] can be seen for a review of these techniques.

On the other hand, several new studies including those on POBREP have tried to bring together process knowledge and multivariate SPC techniques to provide better problem diagnosis. Apley and Shi [8] and Lee and Apley [9] can be seen for factor analysis approaches, Mason and Young [10] for principle components and Ding et al. [11] for an independent-component analysis. Also Apley and Lee [12], Apley and Shi [8] and Jin and Zhou [13] developed methods to extract and identify fault patterns from historical multivariate data.

The POBREP methodology is based on the assumption that process errors (causes) can be linked with resulting pattern of errors over the surface of a manufactured part. Suppose that it is possible to identify a pattern of errors for each potential cause of process bias or variability. Suppose that k different patterns of interest can be identified for k different process causes, say $\mathbf{a}_1$, $\mathbf{a}_2$,..., $\mathbf{a}_k$, where $\mathbf{a}_i$'s are m dimensional vectors. If the vectors $\mathbf{a}_1$, $\mathbf{a}_2$,..., $\mathbf{a}_k$ are independent and $m = k$, then the cause related patterns provide an alternative basis for representing the same quality vector, and the representation of $\mathbf{x}$ in this basis is $\mathbf{x} = z_1\mathbf{a}_1 + z_2\mathbf{a}_2 + \ldots + z_k\mathbf{a}_k$. That is, $\mathbf{x}$ can be thought of as a weighted sum of characteristic patterns, where the amount of pattern $\mathbf{a}_i$ in $\mathbf{x}$ is indicated by the coefficient z_i. The vector $\mathbf{z} = (z_1, z_2, \ldots, z_k)'$ can be found by solving the system of linear equations

$$\mathbf{x} = \mathbf{A}\,\mathbf{z}, \tag{1}$$

where A is the matrix of column vectors $\mathbf{a}_1$, $\mathbf{a}_2$,..., $\mathbf{a}_k$:

$$\mathbf{A} = [\mathbf{a}_1 \mid \mathbf{a}_2 \mid \ldots \mid \mathbf{a}_k]. \tag{2}$$

This basis, $\{ \mathbf{a}_1, \mathbf{a}_2,..., \mathbf{a}_k \}$, is called a process-oriented basis, and each $\mathbf{a}_i$ is called a basis element. By decomposing the observed quality vector, $\mathbf{x}$, into patterns corresponding to known causes, i.e. by solving the system of linear equations to find the $\mathbf{z}$ vector, a process-oriented basis representation is formed. The components of the $\mathbf{z}$ vector, z_i, i = 1,..., k, are called POBREP coefficients. Using the process-oriented basis representation $\mathbf{z}$, diagnosis is possible: potential causes are associated with patterns ($\mathbf{a}_i$) having large positive or negative POBREP coefficients (z_i).

Note that in many cases it will not be necessary to construct a complete basis. This corresponds to a situation where $k < m$. Then, the process-oriented basis may not span the subspace that $\mathbf{x}$ lies in, hence there may be no solution to Equation 1. In this situation, $\mathbf{x}$ can be represented as a linear combination of k basis elements and a residual vector in the following regression equation form:

$$\mathbf{x} = \mathbf{A}\,\mathbf{z} + \mathbf{e} \qquad (3)$$

which can be solved by the least squares method. However, the POBREP methodology differs from the traditional regression context in that Equation 3 is solved for many consecutive quality vectors, and this allows analyzing the behavior of $\mathbf{z}$ and $\mathbf{e}$ over time. Also, statistical properties of POBREP coefficients are different. The probability model in multiple linear regression is

$$\mathbf{X} = \mathbf{A}\,\mathbf{z_0} + \boldsymbol{\varepsilon}, \qquad (4)$$

where $\boldsymbol{\varepsilon} \sim N(\mathbf{0}, \sigma^2\mathbf{I})$, $\mathbf{I}$ is the identity matrix, $\mathbf{0}$ is the zero vector, and $\mathbf{z_0}$ is a fixed but unknown parameter vector; $\mathbf{z}$ coming from the least squares solution of Equation 3 is an estimate of $\mathbf{z_0}$. In POBREP context, however, it is more realistic to assume that the components of $\mathbf{z_0}$, z_{0i}, are themselves random variables, since, in general, problems associated with basis elements will exist in each product with varying degrees. In this case, $\mathbf{z_0}$ represents the true levels of problems associated with the basis elements, and $\mathbf{z}$ from the solution of Equation 3 will give an estimate for the realizations of $\mathbf{z_0}$ in a least squares sense. The POBREP methodology monitors the estimated values z_i in place of z_{0i}.

It is reasonable to assume that the randomness associated with each z_{0i} is a result of the common cause randomness in the process problem or problems associated with z_{0i}. Also the vector $\boldsymbol{\varepsilon}$, models the common cause variations that do not act on basis elements for the specified process problems. By solving Equation 3, $\mathbf{x}$ is represented in terms of the basis elements in a least squares sense where $\mathbf{e}$ represents the part of $\mathbf{x}$ that cannot be explained by the basis elements. Therefore, $\mathbf{e}$ should be considered as an estimate of $\boldsymbol{\varepsilon}$.

The in-control state of a process in POBREP setting can be defined as follows according to the above assumptions: The multivariate quality vector is produced by the probability model in Equation 4 such that each z_{0i} and $\boldsymbol{\varepsilon}$, has a stable distribution. Thus, an in-control process might have POBREP coefficients with stable distributions but with large means and/or large variances. This situation concerns the capability of the process rather than the in-control state of the process.

Identification of process errors and generation of fault patterns in the form of a process-oriented basis can be a difficult task; moreover, generation of a basis characterizing process problems correctly and enabling easy interpretation is crucial for a successful POBREP application. The application discussed in this study involves certain difficulties in this respect. The application has been performed to a drilling operation used at an airframe manufacturing plant of an

Kırıkkale University-Faculty of Engineering

airplane manufacturer. Airframe manufacturing involves processing of sheet metals and assembly operations at various stages of airplane production. The operation involves drilling multiple side and top holes to stringers, which are long aluminum strips used in fuselage and wing assembly of an airplane. Drilled holes are measured using a vision system for location errors, providing multivariate quality data for the application of POBREP. The work completed on this application includes investigating the operation and potential error causes, determining the sorts of problems that the POBREP methodology can be applied, constructing the basis elements for some of these problems, analyzing production data by graphical methods for detecting patterns that can be linked with the specified problems, and applying the POBREP methodology to production data.

The difficulties in the application of the POBREP methodology are twofold. First, high complexity of the CNC machining process poses substantial basis modeling problems. Second, the quality vector $\mathbf{x}$, may have varying dimensions changing from one product to the next on the production line, which is uncommon for many manufacturing settings. Therefore this study gives special emphasis to these issues. Further, it elaborates on modeling issues in order to help solve modeling problems in similar and probably less complex CNC machining operations.

The following section provides an overview of the drilling operation and a description of the associated problems. Section III explains the stringer drilling operation and Section IV discusses in detail the quality problems that have been experienced. Sections V, VI and VII describe how the POBREP methodology can be applied for diagnosing the causes of the observed errors in this particular setting. Section VIII includes the application of the methodology to production data. Finally Section IX provides some conclusions.

II. Stringer Drilling and Associated Problems

This operation involves drilling stringers on an NC machine. Stringers are thin metal strips with varying lengths from 2 to 32 feet, and their cross-sections resemble either a U shape or an L shape. A stringer with a U shape cross-section is called a *hat-section stringer*, and similarly a stringer with an L shape is called a *Z-section stringer*. Figure 1 illustrates a hat-section stringer with 3 holes on both sides and 3 holes on the top. The NC machine drills side holes and top holes along the length of a stringer starting from one end of the stringer and moving to the other. The quality characteristic that is inspected is the positioning of hole centers, that is, center coordinates of each hole is measured and compared with the nominal values.
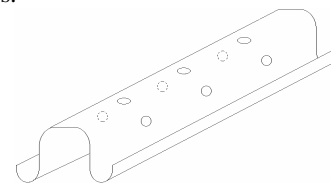

Fig 1. A Hat-section Stringer

Another quality characteristic that is of concern is the diameter of the holes but the current inspection system does not allow an accurate measurement of the hole diameters, hence, this characteristic is not currently monitored. The inspection is performed through a vision system that is mounted near the drill tip; when a hole is drilled the vision system takes a picture of the hole and a software program analyzes the picture and reports the hole center deviations. There are different types of problems that produce deviations from the nominal hole coordinates:

(i) The NC machine works on a major axis of 35 feet to accommodate large stringers. Moreover, stringers may have different types of contours and the NC machine has to accommodate for these contours as well; this is achieved via a complex machine structure that controls 9 movement axes. Because of the major axis length and the machine complexity, the machine experiences problems due to geometry-related calibration and mechanical and positional calibration. For instance, errors in the straightness of the axis beds or errors in the perpendicularity of two axis beds cause deviation patterns in the drilled hole locations. There are several geometry-related, mechanical and positional characteristics of the machine that are calibrated over a fixed period of time to maintain the error involved in each of these characteristics within small tolerances so that the compound effect of the errors will cause tolerable deviations in the hole locations; this process is called *the re-certification process.* The effect of the miscalibrations on the hole location errors is two-fold: Since the vision system is mounted on the NC machine, the measurements are not free of geometry-related calibration problems. Therefore miscalibration of a geometry-related characteristic may effect not only the drill-tip positioning but also the vision system positioning, giving rise to both machining error and measurement error.

(ii) Shape imperfections in a stringer due to prior bending operation cause the vision system to report a non-existing deviation. This is a major problem for hat-section stringers with thin material. When the *channel-width* of a stringer, the width between the two ends of the U cross-section, is larger than the nominal at a particular location of a stringer, this will not cause an error in the location of a side hole drilled at that location, but the vision system reports an error. This situation arises because the drill tip pushes the side of the stringer to a back support right before drilling takes place, positioning the stringer so that the hole will be drilled at the correct coordinates regardless of the width problem. However, there is no such physical contact when the vision system takes a picture of the drilled hole; this gives rise to a bias in the reported hole coordinates.

(iii) There is a temperature compensation system built in the NC machine as a protection against high temperatures. However, the compensation system involves a bias, and as the ambient temperature goes above a critical temperature

the bias becomes significant, causing errors in the hole locations along the length of a stringer. This problem is known to exist through additional studies, but since the compensation mechanism is used for rescaling both machining and vision system coordinates, the vision system cannot measure the resulting error patterns.

(iv) The initial positioning of a Z-section stringer can cause deviations along the width of the top hole locations because the work supports that hold a stringer are not designed to prevent a shift in the initial positioning of a Z-section stringer along the stinger width. This will cause all the top-hole centers to shift in the same direction.

Among the problems mentioned above, the quality engineers are mostly concerned with the calibration problems (problem (i)): The calibration problems effect all the stringers that are produced unless they are corrected. In contrast, the remaining problems may be significant for one stringer and may not be for another since they depend on the stringer shape (problem (ii)), the ambient temperature (problem (iii)), and how a stringer is initially positioned on work supports (problem (iv)). Also, the machine has to be certified over fixed periods of time due to the strict regulations of the U.S. Federal Aviation Administration (FAA) and several characteristics have to be checked during this process. As an aid to this expensive process, the quality engineers want to be able to detect the particular characteristics that contribute most to the observed deviations using the data obtained from the vision system. In addition, this kind of problem detection will have other benefits such as detecting the characteristics that require re-calibration after a system crash without waiting for the next re-certification. Another related problem is the differentiation between machining and vision system errors resulting from the calibration problems. For instance, if there is strong evidence that the observed error is due the vision system rather than the drill positioning, then this will indicate that the real deviation will be less than what the vision system reports. Therefore, the quality engineers are also interested in developing a differentiation scheme.

In Sections V and VI, the POBREP methodology is proposed as a strategy to detect the characteristics that are significantly contributing to calibration problems. The basis elements are formed by defining the pattern of each characteristic on both measurement and machining errors. These patterns can be identified for several characteristics, particularly for the geometry-related ones. In this context, POBREP will be used for machine calibration diagnosis in which the problem is to diagnose a persistent error source on several consecutive production pieces. In this respect, the use of POBREP will be out of the SPC framework, whereas the problems described in items (ii), (iii) and (iv) require the use of POBREP in a SPC framework, that is, these problems are stringer-dependent rather than machine-dependent.

III. STRINGER DRILLING OPERATION

Stringers are used in the main body of an airplane to connect the airplane skin to the frames. Frames are elliptical structures positioned parallel to each other along the length of

the main body. They form the ribs of an airplane skeleton. Stringers are long aluminum strips that lie across the frames establishing the connection between the skin and the frames. The skin connection is established through riveting the top holes of a stringer to the holes on the skin. For frame connection, the side holes of a stringer are fastened to the holes on an intermediate component called clip, and the clip holes are fastened to the holes in the frames. Therefore it is very important that the holes on any two components to be fastened match each other, and this requires keeping the error involved in stringer drilling within tight tolerances. Figure 2 illustrates the cross-sections of a hat-section and a Z-section stringer, and their respective top and side hole locations.

There are more than one hundred stringer types differing in length, contours and the locations of the holes as well as in cross-sections. For instance, stringer length varies from 2 feet to 32 feet, and there is an average of 4 holes drilled per 20 inches along a stringer while the hole locations change from stringer type to stringer type. Most of the stringer types are hat-section stringers, hence most of the discussion here will be based on processing of hat-section stringers.

The Ingersoll 9-Axis AC Stringer Drill was designed by the Ingersoll Company for the stringer drilling process which was previously performed manually. When the application was performed, there were two of these drills at the airframe manufacturing plant; one had been used for more than two years and the other was installed and started production a couple of months before the application. From this point on, all the discussion refers to the old drill except for an explicit mention of the new drill in Section IV and Section VII.
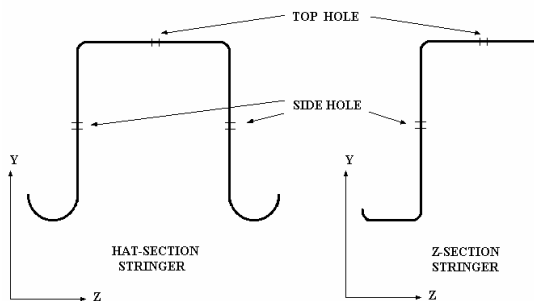
Fig 2. Cross-sections of Hat-section and Z-section Stringers

The machine is shown in Figure 3. It has 9 axes, namely X, Y, Z, A, B, C, V, W and E. Among them, A, B, C and E are rotational axes. A stringer is placed on work supports along the X-axis with one end starting from either work support 1 or work support 21. The X-axis corresponds to moving along the length of a stringer. The Y-axis is used in the initial positioning of the drill on a particular drill location and the Z-axis is for positioning the drill tip on the desired Z location. The A, B and C axes are used for accommodating the drill approach angle to different contours along the stringer. The axes Y and Z in Figure 2 indicate how a stringer is positioned on work supports with respect to the axes. In this figure, the X-axis goes through the picture. Although top and side holes all appear in Figure 2, they do not necessarily have the same X-axis coordinate.

The V, W, and E axes handle movement of the drill tip, movement of the camera, and positioning the drill for side holes and top holes. Figure 4 and 5 illustrate the initial positioning of the drill for drilling a top hole and a side hole, respectively. As can be seen from the figures, the drill tip and the camera are mounted to the same piece, which moves around the rotational axis E. For drilling a top hole, the E-axis bed itself moves down along the V-axis, and moves up after the drilling is done. Next, the camera is positioned at right angles with the drilled hole by a movement of the E-axis bed to the left along the W-axis. Then the camera takes a picture of the hole, and the E-axis bed goes back to its initial position. A similar sequence is repeated for side holes: as shown in Figure 5, the drill tip is positioned at right angles with the side hole position. Movement of the E-axis bed along the W-axis moves the drill into and out of the stringer and the movement along V-axis positions the camera at right angle with the hole.
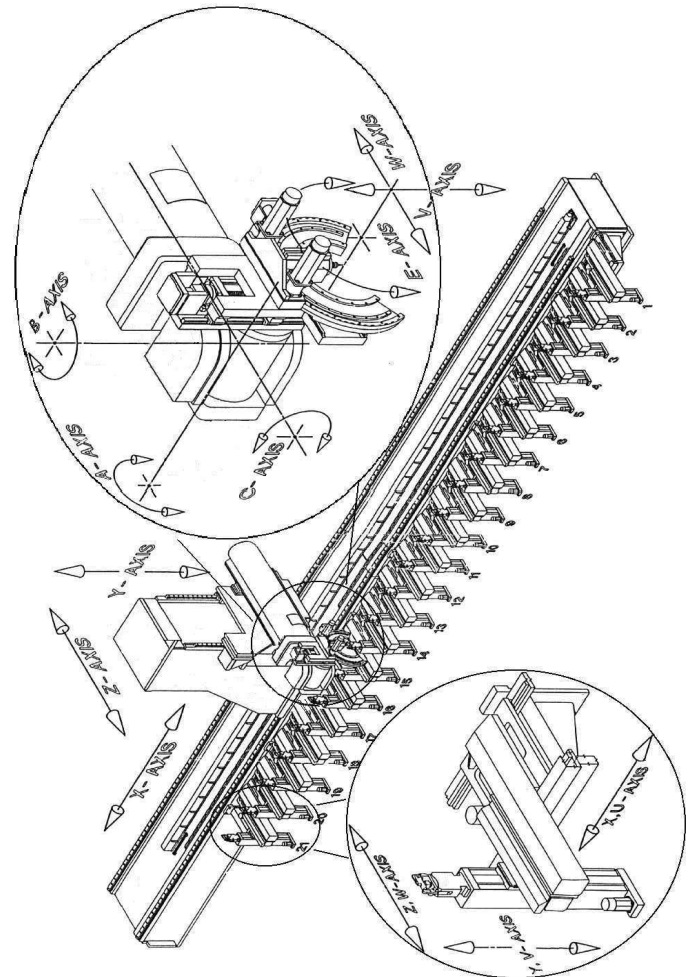
Fig 3. Ingersoll 9-Axis AC Stringer Drill

In addition to the movement of the camera and the drill tip in 9 axes, the work supports can also move along the X, Y and Z axes as shown in Figure 3. Before a stringer is initially positioned on the work supports, the CNC program for the particular stringer type is loaded and the work supports are

positioned in X, Y and Z so as to accommodate for the length and contours of the stringer type. Another important consideration is to position the work supports so that the holes to be drilled remain between any two work supports, not in the vicinity of any. This has an obvious reason: work supports do not tighten the stringer, rather, this is accomplished by a clamping mechanism that tightens the stringer at the point of drill before the drilling takes place. The tightening mechanism has two elements: an upper piece which pushes the stringer from the top at a point close to the hole position, and a cubic piece, called button, which goes into the rectangular area of a hat-section stringer (or the semi-rectangular area in a Z-section stringer) and fixes the stringer at the hole position. When the drill tip goes through the stringer it actually goes into holes in the button.
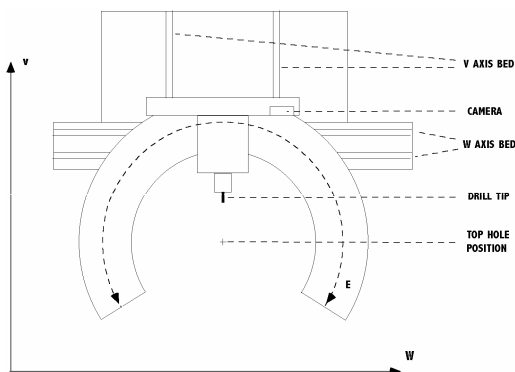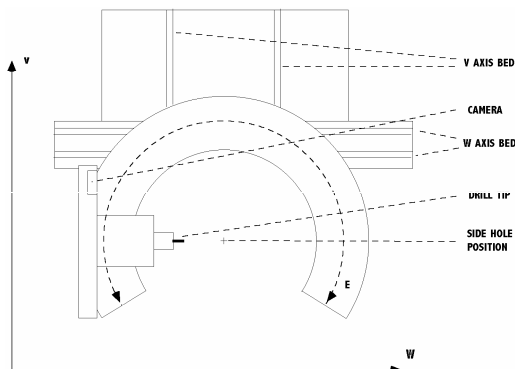

Fig 4. Drilling a Top Hole

Fig 5. Drilling a Side Hole

IV. QUALITY PROBLEMS

A. Geometry-Related, Mechanical and Positional Problems

The complexity of the stringer drill brings with it problems associated with the machine geometry, and the positional and mechanical aspects of the machine. Ingersoll and the airframe manufacturing plant developed a test procedure to maintain the calibration of the machine with respect to several characteristics. This procedure is called the *Re-certification Process*, which was repeated once in every 120 days. Certification is required to allow manufacturing and quality assurance to utilize the capabilities of the machine for final product acceptance of hole locations and diameters. The re-certification process requires taking the

machine off-line for about 6 days. It includes testing 39 different characteristics using experimental setups that are independent of the machine characteristics, for instance, laser interferometers are used as a part of some of these setups. Next, adjustments are made to reduce the observed problems, and subsequent measurements are taken if necessary to assess improvements as a result of the adjustments and finally an artifact test is performed to measure the on-line capability of the machine.

Some examples from the re-certification tests are;
(i)   X-axis straightness of travel with respect to Z-axis and Y-axis,
(ii) Z-axis perpendicularity to X-axis travel (Z-axis straightness of travel with respect to X-axis),
(iii) Z-axis perpendicularity to Y-axis,
(iv) W-axis parallelism to Z-axis,
(v)   Spindle centerline parallelism to W-axis,
(vi) Flatness and X-axis deviation of A-axis plane of rotation,
(vii) X-axis positioning accuracy and repeatability.

Tolerances are computed for each of the 39 characteristics, for instance, suppose that Z-axis perpendicularity to the Y-axis is measured as $0.0012''$ in one re-certification study. If these tolerances are greater than pre-specified tolerances, then adjustments are made to bring the machine within tolerance.

For each characteristic, engineering knows how to calibrate the machine so that the errors will be small. This requires a detailed knowledge of the geometry and the mechanical characteristics of the machine. However, a statistical model linking the observed tolerances in re-certification tests into the tolerances of hole locations and diameters has not been developed yet. The quality engineering team previously attempted to develop such a model in collaboration with some consultant companies, but they were not able to build one because of the mathematical complexity involved. Instead, they take advantage of a final study after all the measurement tests and calibrations are performed in the re-certification process. 'Artifacts', that is, pre-drilled and certified stringers, are used to measure the vision system capabilities of the machine. An artifact study involves positioning an artifact on the work supports and running the machine. The machine does not have a tool in this study, but the drill tip moves as if it drills a hole, and then the camera takes pictures of the pre-drilled hole. Although this study gives information about the vision measurement capability, it does not measure the machining capability. Measuring the machining capability requires drilling artifacts and certifying them in a coordinate measurement machine (CMM) machine. This way, hole coordinates that are fed to the drill, the coordinates reported by the vision system and the actual coordinates of the drilled holes would be available to evaluate both the machining and vision system capabilities. However, this is an expensive process, hence, is not currently implemented.

A common feature of the problems mentioned in this section is that they are all machine-dependent, hence they

introduce systematic errors that persist over stringers that are machined between two consecutive re-certification periods unless a significant change happens in the characteristics. Since many of the characteristics are likely to generate systematic error patterns, it can be conjectured that these patterns will be noticeable in the real production data if the magnitude of the systematic errors are comparable to the magnitude of the errors coming from other sources. The quality engineers were observing such patterns on the individual control charts in the real production data as well as in the artifact studies. However the patterns are not clear from these charts, and there is no way of checking whether the patterns are changing over time.

Multiple stem and leaf plots are proposed as an alternative graphical representation for getting a better picture of the error patterns. Three stringer types are selected for this study and the same method is also applied to several artifact data sets for the newly installed stringer drill. All the plots revealed dominant error patterns. Figures 6 and 7 illustrate two of the plots for one of the artifact data set. There are 9 observations for each hole in the data set for the same artifact. Minus and plus signs indicate the holes belonging to two different sides of the artifact. There are a total of 7 hole pairs across from each other along the X-axis of the stringer. Both of the figures reveal a pattern for each hole pair: the hole which is on the minus side has a bigger error value than the hole on the other side. There is also a noticeable trend across the X-axis in both plots. Multiple stem and leaf plots make it possible to compare the empirical distributions of the errors for different holes. For instance, the graphs in Figures 6 and 7 indicate that the underlying distribution does not change significantly from one hole to the other. Interestingly, similar plots are obtained from the stringer data machined on the first stringer drill. In this case, there is one observation per hole for each stringer, and the plots are obtained for multiple stringers of the same type. The plots obtained from the stringers show that the patterns prevail over several stringers. Therefore there is strong evidence that they stem from a machine-dependent (camera or machine setup error) problem. For instance, the patterns regarding two facing side holes in Figure 6 are also observed in the X versus X-deviation plots for the stringers examined. The quality engineers link this pattern to a possible parallelism problem between the A-axis rotation plane and the E-axis rotation plane.
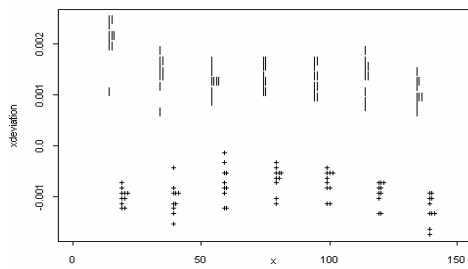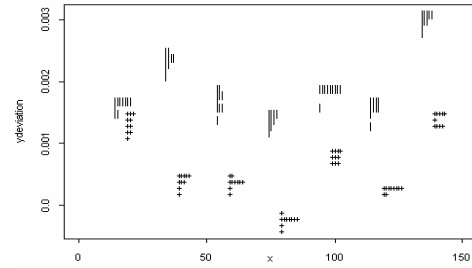

Fig 6. X-axis Deviations for Side Holes

Fig 7. Y-axis Deviations for Side Holes

The quality engineers predict the potential root causes for the patterns observed in the real data using their past expertise with the machine, but the test results from the re-certification process help them little in this regard, because the observed patterns are the compound result of several problems.

One drawback of the re-certification process for measuring the process capability of the machine is that it is repeated once in every 120 days, therefore, any change in the tolerances of the 39 characteristics will not be observed during the real-time production. Consequently, new problems will only be discovered in the next re-certification study. On the other hand, the production data is likely to give some insights about such changes in the observed position errors.

There is a further complication about examining the production data. Since the vision system and the drill tip are mounted on the same piece, they are both subject to the effects of the problems in several of the 39 characteristics, and this is particularly true for geometry-related problems. In this case, the error reported by the camera will be not be pure camera error or the pure machining error, but a confounded version of both of them. On the other hand, artifact studies will reveal the pure camera error involved for the pre-drilled artifact.

In conclusion, the major difficulties regarding the machine-dependent problems are as follows:
(i) Detecting the root causes for the systematic errors from the production data,
(ii) Differentiating between the camera error and machining error in the production data,
(iii) Linking the tolerances observed in the re-certification tests to the tolerances of hole locations with regard to measurement and machining error.

B. Problems Related to Stringer Shape

A stringer is given its cross-sectional shape through a forming process. A crucial step in this process is to bend the stringer so that the channel width, the width of a stringer along Z-axis at the bottom part of a stringer in Figure 2, is precise. However, this is not accomplished in reality; instead, the channel width is usually larger than the target value. This is a common problem for the stringer types with thin aluminum material. As a corrective step, the operators measure the channel width at multiple locations along a stringer after the forming, and if the channel width is larger than the target value at a location, they manually hammer the

stringer from both sides to get it closer to the target value. The manual correction results in better channel widths, but the channel width varies along the stringer in this case. In addition, errors usually remain positive, that is, the channel widths are still larger than the target values, because the operators try not to bend the stringers beyond the target value, in order to avoid any problems with the clamping mechanism in the drill.

Varying channel widths gives rise to a measurement problem in drilling. When the channel width is larger than the target value at a hole location of a stringer, the sides of the stringer does not make a 90-degree angle with the top, instead the angle is slightly larger than 90 degrees. This situation holds when the stringer is positioned on work supports and clamped for drilling. When a side hole is drilled, the drill tip first pushes the side until it is tightly supported by the button at the back, giving it a perfect 90-degree angle shape. This is the correct angle a stringer will assume when assembled on an airplane body. Next, the drill tip retracts, relaxing the side of the stringer back to its original angle. Only then the vision system takes a picture of the hole. Consequently, the measured Y coordinate of the side hole turns out to be slightly larger than it was when the side was making a 90-degree angle. In this case, for instance, if the hole were drilled at the exact coordinates, the vision system would incorrectly report a positive Y-axis deviation.

This problem introduces a bias in the measurements that vary in degree along a stringer that has been manually re-bent. The more severe the channel width problem is at a hole position, the larger the positive Y-axis bias will be in the measurement. A corrective measure that was taken recently was to manually bend the stringers further after the forming process. At this point, it is not known how much this measure has reduced the problem.

C. Problems Related to Ambient Temperature

This problem is about the effect of high ambient temperatures experienced during hot summer days. High ambient temperatures increase the temperature of a stringer that is being machined, causing the aluminum stringer to elongate. There is a temperature compensation system built in the stringer drill which measures the temperatures of the stringer at the contact points of the work supports via thermosensors. Then an automatic calibration algorithm compensates for the effect of high temperatures by changing the coordinate scale. The reference temperature is 68 °F for which there is no rescaling involved. Furthermore there is no problem with temperatures below 68 °F because the shopfloor environment is heated on cold days. The compensation is done by calculating a coefficient of compensation using the coefficient of expansion of the stringer material. However, this compensation scheme does not work correctly; it either over- or under-compensates. The quality engineers think that this error is due to the slight differences among the composition of the stringer materials, which change the coefficient of expansion from stringer to stringer, whereas the algorithm uses the coefficient of expansion of an ideal

stringer material. Therefore the difference between the coefficient of expansions will generate either over- or under-compensation, resulting in drilling holes at wrong X-coordinates.

The machining and the vision system coordinates are subject to the same rescaling by the temperature compensation system, which makes it impossible to observe the effect of incorrect compensation in the vision system data. This effect was first observed in artifact studies performed on a CMM machine. The effect of the high temperatures was quantified in this study to take corrective action for further use of the same stringer artifacts. It was observed in this study that the temperatures above 90 °F caused significant effects of over- or under-compensation. This happens only for a short period during summer season in a production year. Moreover, this effect becomes significant only along the length of a stringer (X-axis), since the width (Z-axis), and the height (Y-axis) are too short for an error in the coefficient of expansion to cause a significant machining error.

D. Problems Related to Ambient Temperature

When a Z-section stringer is positioned on the work supports, the side of the Z-section stringer might not make a full contact with the button: there is no mechanism to make sure that full contact is established. This causes a Z-axis positioning error for the top holes, whereas the effect is negligible for the side holes. This problem does not occur for hat-section stringers because the button fits between the side surfaces, which prevents any problem of shift in Z-axis. The problem is dealt with by manually checking the stringer positioning at each drill location before a new hole is drilled. This solution seems to reduce the degree of the problem in recent production data.

V. A GENERAL FRAMEWORK FOR POBREP MODELING

Section IV examined major sources of machining and vision system errors experienced in the stringer drill. Among them, machine-dependent problems (section IV.A) constitute a suitable application area for the POBREP methodology. The POBREP methodology decomposes an error vector into distinct error patterns, each of which can be linked to one or more error sources. Many of the mechanical and geometry-related problems that are resulting in the calibration problems in the re-certification tests can be regarded as one such error source, which is generating error patterns in terms of errors in multiple hole locations on a stringer.

It can be reasonably assumed that each problem regarding a mechanical or geometry-related characteristic of the drill will induce an error pattern on the coordinates of the drilled holes and on the vision system measurements. If a generic error pattern can be found for each of the problems then the following statistical model can be used for the decomposition of the observed errors:

$$\mathbf{c}_e = p_1\mathbf{c}_1 + p_2\mathbf{c}_2 + \ldots + p_n\mathbf{c}_n + \mathbf{e}_c, \tag{5}$$
$$\mathbf{m}_e = r_1\mathbf{m}_1 + r_2\mathbf{m}_2 + \ldots + r_n\mathbf{c}_n + \mathbf{e}_m, \tag{6}$$

where

c_e : Observed camera error vector,

c_i : Camera error pattern for problem i,

m_e : Observed machining error vector,

m_i : Machining error pattern for problem i,

e_m : Residual vector for machining error,

e_c : Residual vector for camera error,

p_i : Regression coefficient for c_i, and

r_i : Regression coefficient for m_i.

In this notation, each element of the vectors represents the error along one axis in one hole. Models in Equations (5) and (6) are equivalent to the POBREP model in Equation (3), hence, c_i and m_i can be considered as the process-oriented basis elements for camera and machining problems.

There are two problems associated with these models. One is that it is not possible to model certain problem types such as flatness. Flatness problems, for example, might arise in several ways, hence there is no single basis element that can represent flatness error. Nevertheless it is very conceivable that such generic basis elements can be generated for perpendicularity and parallelism problems. It is also possible to associate certain error patterns with positional errors due to stepper motors that are governing the 9 axes.

Another problem is that although c_e is available from the vision system data, m_e is not. The machining error m_e can be measured only if the actual coordinates of a drilled hole are available. The actual coordinates can be measured on a CMM machine assuming that the error due to the CMM machine is negligible. Figure 8 illustrates a situation when actual coordinate of a single hole for a particular dimension is available (from a CMM study). In this figure NOMINAL indicates the hole coordinate fed to the drill, CAMERA indicates the measured coordinate of the hole, and ACTUAL indicates the actual coordinate of the hole. We define the camera error as the deviation of the reported coordinate from the actual coordinate. Therefore, Camera Error = CAMERA - ACTUAL, and Machining Error = ACTUAL - NOMINAL. As illustrated in Figure 8, the error reported by the camera is not the pure camera error. Let Reported Error = CAMERA − NOMINAL. Then, Camera Error = Machining Error + Reported Error.

The application of the POBREP methodology involves generating the process-oriented basis elements for camera and machining error. We develop 20 basis elements in section VI, however, there are still remaining problems that can be modeled and added to the basis in future studies.
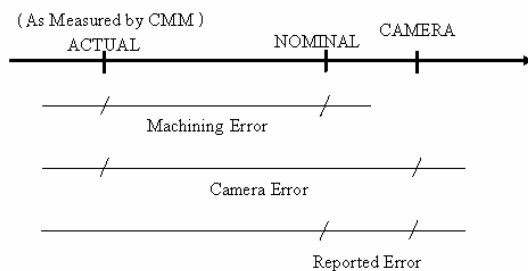

Fig 8. Nominal, Actual and Camera-reported Hole Coordinates

Kırıkkale University-Faculty of Engineering

VI. CONSTRUCTION OF PROCESS-ORIENTED BASIS ELEMENTS

We first discuss POBREP modeling of two geometry-related problems and a problem related with the stringer shape in Sections VI.A to VI.C. These problems were considered as the most significant contributors to the error patterns observed in the production data during the time of the application.

As mentioned in Section IV.A, there might be many possible sources of mechanical and geometry-related problems. Section VI.D includes modeling mechanical positional problems due to stepper motors which govern the movement of the 9 axes, and Section VI.E includes modeling some problems due to lack of perpendicularity. Section VI.F considers problems due to initial positioning error of the camera, and finally Section VI.G considers modeling the ambient temperature problem of Section IV.C.

As explained in Section IV.C, it is not possible to observe the effect of the ambient temperature in the current situation. However, if the means were available to measure the correct coordinates of the drilled holes, such as by taking CMM measurements at the reference temperature, the patterns resulting from production at high temperatures could be modeled as a process-oriented basis element. The modeling will be provided under the assumption that the correct hole coordinates are available for the reference temperature.

Since there are hundreds of different stringer types and each type differs in shape, hole number and hole coordinates, it is necessary to generate a process-oriented basis for each stringer type (c_i and m_i, $i = 1,..., n$, in Equations 5 and 6). Nevertheless, this is a simple task and a computer routine can be written to generate the basis for each stringer type with respect to the orientation and coordinates of the holes.

For illustration purposes, the process-oriented basis elements will be generated for a hypothetical hat-section stringer type with 9 holes, which is illustrated in Figure 1. There are two side holes facing each other and a top hole at one X location of the stringer type, and there are 3 such X locations with 3 holes at each one. Then the following vector notation of hole coordinates will suffice to describe the stringer type for POBREP modeling:

$$(x_1, y_1, x_2, z_2, x_3, y_3, x_4, y_4, x_5, z_5,$$
$$x_6, y_6, x_7, y_7, x_8, z_8, x_9, y_9)' \qquad (7)$$

To be more specific about the coordinate frames, X coordinate increases with the increasing number of work supports along the X bed, Y coordinate increases as the position physically gets higher, and Z coordinate increases from left to right when observed from the side of the drill with the work-support 1. In the notation of (7), subscripts, $i = 1,..., 9$ denote the hole numbers; the holes 1, 2 and 3 are at the same X coordinate and so are the holes 4, 5 and 6, and the holes 7, 8 and 9. Therefore $x_1 = x_2 = x_3$, $x_4 = x_5 = x_6$, and $x_7 = x_8 = x_9$. Furthermore, the holes 2, 5 and 8 are top holes, holes 1, 4 and 7 are near-side holes, and holes 3, 6 and 9 are far-side holes. The choice of near-side and far-side is with respect to the machine and arbitrary. For instance, the side holes with

positive Z coordinates may be considered far-side holes, and similarly the side holes with negative Z coordinates may be considered near-side holes since the Z axis is defined with respect to the stringer drill.

Because the POBREP models in Equations 5 and 6 include errors rather than the real coordinates, the vectors c_e, m_e, c_i, and m_i, i = 1,..., n, in these equations are denoted as follows:

$$(\Delta x_1, \Delta y_1, \Delta x_2, \Delta z_2, \Delta x_3, \Delta y_3, \Delta x_4, \Delta y_4, \Delta x_5, \Delta z_5, \\ \Delta x_6, \Delta y_6, \Delta x_7, \Delta y_7, \Delta x_8, \Delta z_8, \Delta x_9, \Delta y_9)' \quad (8)$$

In this notation, the symbol Δ represents the difference from the correct coordinate value. For example, the first component of the observed machining error vector m_e, Δx_1, is the machining error in the X coordinate of the hole 1.

A. Modeling a Parallelism Problem between the A-axis and the E-axis Rotation

This problem arises when the E-axis bed is not parallel to the A-axis rotation plane. The suspected parallelism error is in the form of the rotation of the E-axis bed with respect to an axis that is parallel to the V-axis and passing through the center of the circle that E-axis bed defines (see Figure 4). This causes an error in the X coordinates of the side holes which is changing sign from one side to the other. The drill tip and the camera are both subject to the problem when the side holes drilled. Denoting this problem by $i = 1$, the following vectors will be the process-oriented basis elements for the camera and the machining;

$$c_1 = (1, 0, 0, 0, -1, 0, 1, 0, 0, 0, -1, 0, 1, 0, 0, 0, -1, 0)', \quad (9)$$
$$m_1 = (1, 0, 0, 0, -1, 0, 1, 0, 0, 0, -1, 0, 1, 0, 0, 0, -1, 0)'. \quad (10)$$

When these basis elements are applied to production data, sign of the POBREP coefficients will reveal the direction of the E-axis bed rotation.

The current situation in the stringer drill requires refinements on the basis elements given in Equations (9) and (10). The stringer is not placed at the center of the E-axis bed as shown in Figure 4, but to the left of the center. This asymmetry causes the magnitudes of the errors on near and far sides to differ. Another effect of the asymmetry will be an error on the X coordinates of the top holes, however this error will be small enough to be safely ignored. Using the particular machine geometry, it is possible to compute the differences between two sides which will lead to the following process-oriented basis elements:

$$c_1 = (1, 0, 0, 0, -k, 0, 1, 0, 0, 0, -k, 0, 1, 0, 0, 0, -k, 0)', \quad (11)$$
$$m_1 = (1, 0, 0, 0, -k, 0, 1, 0, 0, 0, -k, 0, 1, 0, 0, 0, -k, 0)', \quad (12)$$

where k is an unknown constant to be found from the machine geometry. The center of the E-axis bed, the position of the holes prior to drilling, and the diameter of the E-axis bed can be used to compute k. If it is not possible to compute

k, an alternative process-oriented basis representation can be used where one error pattern is represented by two vectors instead of one:

$$c_{11} = (1, 0, 0, 0, -1, 0, 1, 0, 0, 0, -1, 0, 1, 0, 0, 0, -1, 0)', \quad (13)$$
$$c_{12} = (0, 0, 0, 0, -1, 0, 0, 0, 0, 0, -1, 0, 0, 0, 0, 0, -1, 0)', \quad (14)$$
$$m_{11} = (1, 0, 0, 0, -1, 0, 1, 0, 0, 0, -1, 0, 1, 0, 0, 0, -1, 0)', \quad (15)$$
$$m_{12} = (0, 0, 0, 0, -1, 0, 0, 0, 0, 0, -1, 0, 0, 0, 0, 0, -1, 0)'. \quad (16)$$

Here, the ratio of the POBREP coefficients $(z_{11} + y_{11})/z_{11}$ is expected to give an estimate of the unknown coefficient k.

B. Problem due to Orientation of the Drill Tip and the Camera

The particular problem is caused by the mis-orientation of the mechanical piece that holds the camera and the drill tip with respect to the E-axis rotation bed. Figure 4 shows the piece such that the drill tip points at the location of a top hole. If the piece is tilted toward right or left, the drill tip does not point at this location anymore. This causes an error in the Y coordinates of the side holes and an error in the Z coordinate of the top holes. As in section VI.A the basis elements for the camera and machining errors will be the same. Denoting this problem by $i = 2$, the basis element will be as follows:

$$c_2 = (0, 1, 0, t, 0, -1, 0, 1, 0, t, 0, -1, 0, 1, 0, t, 0, -1)', \quad (17)$$
$$m_2 = (0, 1, 0, t, 0, -1, 0, 1, 0, t, 0, -1, 0, 1, 0, t, 0, -1)', \quad (18)$$

where t is either 1 or -1 according to the particular direction of the tilt (let or right in Figure 4). If the engineering is not sure about the direction, two basis elements with $t = 1$ and -1 can be tried in Equations (1) and (2); the one with a consistently bigger POBREP coefficient will be the correct basis element to use. This will also reveal the direction of the tilt.

A complication arises from the fact the camera and the drill tip are calibrated positionally in the re-certification studies, and there are no consistent error patterns for the top holes in the production data. This necessitates setting $t = 0$ in Equations (17) and (18). Alternatively, if consistent errors for the top holes are suspected from the particular problem in spite of the calibration two basis elements can be used as in section VI.A:

$$c_{21} = (0, 1, 0, 0, 0, -1, 0, 1, 0, 0, 0, -1, 0, 1, 0, 0, 0, -1)', \quad (19)$$
$$c_{22} = (0, 0, 0, 1, 0, 0, 0, 0, 0, 1, 0, 0, 0, 0, 0, 1, 0, 0)', \quad (20)$$
$$m_{21} = (0, 1, 0, 0, 0, -1, 0, 1, 0, 0, 0, -1, 0, 1, 0, 0, 0, -1)', \quad (21)$$
$$m_{22} = (0, 0, 0, 1, 0, 0, 0, 0, 0, 1, 0, 0, 0, 0, 0, 1, 0, 0)'. \quad (22)$$

C. Modeling the Problem Related to Stringer Shape

This problem is described in Section IV.B. The effect is a positive deviation in the Y coordinates of the side holes, but the degree of the problem differs along the length of a stringer. Nevertheless, the following basis element can be used for the resulting camera error; regressing it to the observed camera error c_e in Equation (5) is equivalent to

removing the average of the Y coordinate errors, which are resulting from the shape imperfections, from $\mathbf{c}_e$. Denoting this problem by $i = 3$,

$$\mathbf{c}_3 = (0, 1, 0, 0, 0, 1, 0, 1, 0, 0, 0, 1, 0, 1, 0, 0, 0, 1)'. \qquad (23)$$

D. Mechanical Positional Problems due to Stepper Motors

There are stepper motors governing the movement along 9 axes of the stringer drill. When these motors do not take the exact number of steps to position the drill tip and the camera, problems of accuracy and repeatability arise. We consider only accuracy problems in the form of a persistent bias. For instance, the motor for the X-axis movement always moves the drill tip with a certain bias (positive or negative). The bias for X, Y, Z, V and W axes would be considered in terms of bias in distance, while the bias for A, B, C and E axes would be in terms of bias in angles. We assume that the error does not build up from one hole to the next, instead, always the same amount of bias is observed for consecutive holes. Since, the drill tip and the camera are on the same piece, the camera and machining error patterns are mostly the same. The following is a summary of the error patterns:

(i) X-axis positional bias:
$$\mathbf{c}_4 = (1, 0, 1, 0, 1, 0, 1, 0, 1, 0, 1, 0, 1, 0, 1, 0, 1, 0)', \qquad (24)$$
$$\mathbf{m}_4 = (1, 0, 1, 0, 1, 0, 1, 0, 1, 0, 1, 0, 1, 0, 1, 0, 1, 0)'. \qquad (25)$$

(ii) Y-axis positional bias:
$$\mathbf{c}_5 = (0, 1, 0, 0, 0, 1, 0, 1, 0, 0, 0, 1, 0, 1, 0, 0, 0, 1)', \qquad (26)$$
$$\mathbf{m}_5 = (0, 1, 0, 0, 0, 1, 0, 1, 0, 0, 0, 1, 0, 1, 0, 0, 0, 1)'. \qquad (27)$$

(iii) Z-axis positional bias:
$$\mathbf{c}_6 = (0, 0, 0, 1, 0, 0, 0, 0, 0, 1, 0, 0, 0, 0, 0, 1, 0, 0)', \qquad (28)$$
$$\mathbf{m}_6 = (0, 0, 0, 1, 0, 0, 0, 0, 0, 1, 0, 0, 0, 0, 0, 1, 0, 0)'. \qquad (29)$$

(iv) A-axis positional bias:
$$\mathbf{c}_7 = (0, 1, 0, 1, 0, -1, 0, 1, 0, 1, 0, -1, 0, 1, 0, 1, 0, -1)', \qquad (30)$$
$$\mathbf{m}_7 = (0, 1, 0, 1, 0, -1, 0, 1, 0, 1, 0, -1, 0, 1, 0, 1, 0, -1)'. \qquad (31)$$

This problem can be seen by examining Figures 4 and 5. A bias in A-axis would cause the pieces of the drill shown in the figures to rotate either in clockwise or counter-clockwise directions with respect to a rotation center with the same Z coordinate with the drill-tip (in its top hole drilling position), and a Y coordinate that is above the Y coordinates of the drill tip and the camera.

Note that this formulation sets $\Delta y_1 = 1$, $\Delta z_2 = 1$ and $\Delta y_3 = -1$, hence the bias for the top and side holes have the same magnitude of bias. This is in fact an approximation since Y coordinates of top holes and side holes are very close to each other. Otherwise, the location of the center of rotation would necessitate computing the relative magnitudes of Δy_i and Δz_i's, which would be significantly different.

(v) B-axis positional bias:
$$\mathbf{c}_8 = (0, 0, 0, 1, 0, 0, 0, 0, 0, 1, 0, 0, 0, 0, 0, 1, 0, 0)', \qquad (32)$$
$$\mathbf{m}_8 = (0, 0, 0, 1, 0, 0, 0, 0, 0, 1, 0, 0, 0, 0, 0, 1, 0, 0)'. \qquad (33)$$

Figure 3 shows the effect of this problem. Although this problem affects both X and Z coordinates, the change in the X coordinate, Δx_i, can be ignored as compared to the change in the Z coordinate, Δz_i, for small degrees of deviation.

(vi) C-axis positional bias:
$$\mathbf{c}_9 = (0, 1, 0, 0, 0, 1, 0, 1, 0, 0, 0, 1, 0, 1, 0, 0, 0, 1)', \qquad (34)$$
$$\mathbf{m}_9 = (0, 1, 0, 0, 0, 1, 0, 1, 0, 0, 0, 1, 0, 1, 0, 0, 0, 1)'. \qquad (35)$$

Figure 3 shows the effect of this problem. Although this problem affects both X and Y coordinates, the change in the X coordinate, Δx_i, can be ignored as compared to the change in the Y coordinate, Δy_i, for small degrees of deviation.

(vii) V-axis positional bias: The effect of this problem is the same as the effect of X-axis positional bias.
$$\mathbf{c}_{10} = (1, 0, 1, 0, 1, 0, 1, 0, 1, 0, 1, 0, 1, 0, 1, 0, 1, 0)', \qquad (36)$$
$$\mathbf{m}_{10} = (1, 0, 1, 0, 1, 0, 1, 0, 1, 0, 1, 0, 1, 0, 1, 0, 1, 0)'. \qquad (37)$$

(viii) W-axis positional bias: The effect of this problem is the same as the effect of Z-axis positional bias.
$$\mathbf{c}_{11} = (0, 0, 0, 1, 0, 0, 0, 0, 0, 1, 0, 0, 0, 0, 0, 1, 0, 0)', \qquad (38)$$
$$\mathbf{m}_{11} = (0, 0, 0, 1, 0, 0, 0, 0, 0, 1, 0, 0, 0, 0, 0, 1, 0, 0)'. \qquad (39)$$

(ix) E-axis positional bias: We assume that the bias occurs for every move for drilling side holes, hence there is no bias for the top holes.
$$\mathbf{c}_{12} = (0, 1, 0, 0, 0, 1, 0, 1, 0, 0, 0, 1, 0, 1, 0, 0, 0, 1)', \qquad (40)$$
$$\mathbf{m}_{12} = (0, 1, 0, 0, 0, 1, 0, 1, 0, 0, 0, 1, 0, 1, 0, 0, 0, 1)'. \qquad (41)$$

E. Problems due to Lack of Perpendicularity

This section examines problems due to lack of perpendicularity among X, Y and Z-axis. All of the three cases below consider a fixed amount of errors in terms of degrees of angles. For instance, we assume that Y-axis bed is not perpendicular to X-axis bed in case (i), instead the angle between the two beds is $(90 - \beta)$ degrees regardless of the X-axis coordinate of the Y-axis bed.

(i) Y-axis perpendicularity to X-axis travel: This problem shifts the X and Y coordinates of the holes. However, change in the Y coordinates can be ignored for small β.
$$\mathbf{c}_{13} = (1, 0, 1, 0, 1, 0, 1, 0, 1, 0, 1, 0, 1, 0, 1, 0, 1, 0)', \qquad (42)$$
$$\mathbf{m}_{13} = (1, 0, 1, 0, 1, 0, 1, 0, 1, 0, 1, 0, 1, 0, 1, 0, 1, 0)'. \qquad (43)$$

(ii) Z-axis perpendicularity to X-axis travel: This problem shifts the X and Z coordinates of the holes. However, change in the Z coordinates can be ignored for small β.
$$\mathbf{c}_{14} = (1, 0, 1, 0, 1, 0, 1, 0, 1, 0, 1, 0, 1, 0, 1, 0, 1, 0)', \qquad (44)$$
$$\mathbf{m}_{14} = (1, 0, 1, 0, 1, 0, 1, 0, 1, 0, 1, 0, 1, 0, 1, 0, 1, 0)'. \qquad (45)$$

(iii) Z-axis perpendicularity to Y-axis travel: This problem shifts the Y and Z coordinates of the holes. However, change in the Z coordinates can be ignored for small β.
$$\mathbf{c}_{15} = (0, 1, 0, 0, 0, 1, 0, 1, 0, 0, 0, 1, 0, 1, 0, 0, 0, 1)', \qquad (46)$$

$$\mathbf{m}_{15}= (0, 1, 0, 0, 0, 1, 0, 1, 0, 0, 0, 1, 0, 1, 0, 0, 0, 1)'. \quad (47)$$

F. Problems due to Initial Positioning of the Camera

If the camera is initially mounted at wrong coordinates it will always give readings with a certain amount of bias. We consider X-axis positioning error and Z-axis positioning error separately. Note that when the camera is moved sideways for side holes, Z-axis error affects Y-axis readings.

(i) X-axis camera positioning error:
$$\mathbf{c}_{16} = (1, 0, 1, 0, 1, 0, 1, 0, 1, 0, 1, 0, 1, 0, 1, 0)', \quad (48)$$

(ii) Z-axis camera positioning error:
$$\mathbf{c}_{17} = (0, 1, 0, 1, 0, 1, 0, 1, 0, 1, 0, 1, 0, 1, 0, 1)'. \quad (49)$$

Another type of camera problem arises when the camera angle is not perpendicular to X-Z plane. We consider X-axis and Z-axis perpendicularity problems separately.

(iii) Perpendicularity of camera angle to X-axis:
$$\mathbf{c}_{18} = (1, 0, 1, 0, 1,\ 0, 1, 0, 1, 0, 1,\ 0, 1, 0, 1, 0,\ 0)', \quad (50)$$

(iv) Perpendicularity of camera angle to Z-axis:
$$\mathbf{c}_{19} = (0, 1, 0, 1, 0, -1, 0, 1, 0, 1, 0, -1, 0, 1, 0, 1, 0, -1)'. \quad (51)$$

G. Modeling the Problem Related to Ambient Temperature

This problem is described in Section IV.C in detail. If it were possible to measure the coordinates of the drilled holes by a method that eliminates the bias imposed by the increased temperature, it would be possible to quantify the magnitudes of the camera and machining error caused by the temperature using POBREP. For instance, assume that a stringer is drilled at a high temperature. If the stringer is measured in a CMM machine at relatively low temperatures, i.e. at nighttime, this will substantially reduce the impact of the temperature on the CMM measurements. As a further step, the measurements obtained from the CMM machine can be re-scaled using the coefficient of expansion of a standard stringer and the ambient temperature during the time of CMM measurements.

The effect of high temperature will be significant only along X-axis, since the width and the height of a stringer along the Z- and Y-axes are too short for the temperature to have an effect on the hole coordinates. Assuming that one end of the stringer is fixed to the drill at $x = 0$, and $x_1 < x_4 < x_7$ (Note that $x_1 = x_2 = x_3$, $x_4 = x_5 = x_6$, $x_7 = x_8 = x_9$), then the following are the appropriate basis elements for the camera and the machining error. Letting $r_{41} = x_4 / x_1$ and $r_{71} = x_7 / x_1$,

$$\mathbf{c}_{20} = (1,0,1,0,1,0, r_{41},0, r_{41},0, r_{41},0, r_{71},0, r_{71},0, r_{71},0)', \quad (52)$$
$$\mathbf{m}_{20} = (1,0,1,0,1,0, r_{41},0, r_{41},0, r_{41},0, r_{71},0, r_{71},0, r_{71},0)'. \quad (53)$$

These basis elements are the same, and the resulting POBREP coefficients are also expected to be very close to

each other since the temperature compensation system causes the same error in both the vision system and the drill.

VII. Structure of the Process-Oriented Basis Matrix

Process-oriented basis matrix for the machining problems and the camera problems can be constructed as $\mathbf{A}_m = [\mathbf{m}_1 \mid \mathbf{m}_2 \mid ... \mid \mathbf{m}_{20}]$, and $\mathbf{A}_c = [\mathbf{c}_1 \mid \mathbf{c}_2 \mid ... \mid \mathbf{c}_{20}]$, respectively, using the basis elements developed in Section VI. The basis elements in both $\mathbf{A}_m$ and $\mathbf{A}_c$ have the following property except $\mathbf{m}_{20}$ and $\mathbf{c}_{20}$: the first six components of each vector repeats itself in the remaining components. That is, the error pattern is basically defined by the deviations in one near-side hole, one top hole and one far-side hole. Therefore, the patterns do not change for new holes along the length of a stringer. This is because the main body of the stringer drill moves along X-axis, hence the problems due to other axes are independent of the particular X coordinate of a hole. An exception to this is the basis elements $\mathbf{m}_{20}$ and $\mathbf{c}_{20}$ for the effect of ambient temperature. As explained in Section VI.G, the application of these basis elements is possible only if the effect of the temperature can be measured independently of the stringer drill, which the current production system does not allow. Therefore, $\mathbf{m}_{20}$ and $\mathbf{c}_{20}$ will not be considered in the following discussion.

The basis elements in Section VI are developed for the stringer in Figure 1, but stringers, in general, have varying number of side and top holes at different coordinates. Using the above property, a basis element can be easily generated for any type of stringer by repeating the pattern for one near-side hole for all the near-side holes, and doing the same for the top holes and the far-side holes. This will be illustrated for the artifact stringer in Section VIII. Simplifying the notation in Equation 8, let $(\Delta x_n,\ \Delta y_n,\ \Delta x_t,\ \Delta z_t,\ \Delta x_f,\ \Delta y_f)'$ denote the coordinates of one near-side hole (n), one top hole (t), and one far-side hole (f). Table 1 gives a summary of the basis elements in this format.

Since only six components effectively define a basis element, there can be at most six independent basis elements in both $\mathbf{A}_m$ and $\mathbf{A}_c$. Therefore, Table I includes several linearly dependent basis elements. Finding most of the dependencies is straightforward:

$$\mathbf{a} = \mathbf{m}_4 = \mathbf{m}_{10} = \mathbf{m}_{13} = \mathbf{m}_{14} = \mathbf{c}_4 = \mathbf{c}_{10} = \mathbf{c}_{13} = \mathbf{c}_{14} = \mathbf{c}_{16} = \mathbf{c}_{18},$$
$$\mathbf{b} = \mathbf{c}_{17},$$
$$\mathbf{c} = \mathbf{m}_5 = \mathbf{m}_9 = \mathbf{m}_{12} = \mathbf{m}_{15} = \mathbf{c}_3 = \mathbf{c}_5 = \mathbf{c}_9 = \mathbf{c}_{12} = \mathbf{c}_{15},$$
$$\mathbf{d} = \mathbf{m}_6 = \mathbf{m}_8 = \mathbf{m}_{11} = \mathbf{c}_6 = \mathbf{c}_8 = \mathbf{c}_{11},$$
$$\mathbf{e} = \mathbf{m}_2 = \mathbf{m}_7 = \mathbf{c}_2 = \mathbf{c}_7 = \mathbf{c}_{19},$$
$$\mathbf{f} = \mathbf{m}_1 = \mathbf{c}_1. \quad (54)$$

According to Equation 54, POBREP analysis of machining or camera errors can be performed by a reduced matrix $\mathbf{A}^r = [\mathbf{a} \mid \mathbf{b} \mid ... \mid \mathbf{f}]$. In this situation, finding a significant pattern $\mathbf{a}$ in machining errors from a stringer, for instance, would indicate any of the problems linked with $\mathbf{m}_4$, $\mathbf{m}_{10}$, $\mathbf{m}_{13}$ or $\mathbf{m}_{14}$. As it can be clearly seen from this example, the relatively small number of linearly independent basis

elements reduces the diagnostic power of POBREP methodology. Further, the rank of $\mathbf{A}^r$ is 5, hence $\mathbf{A}^r$ is rank deficient.

TABLE I
GENERIC BASIS ELEMENTS FOR ONE TOP AND TWO SIDE HOLES

Equivalent Basis El.	Generic Basis El.	Deviation in Coordinates					
		Δx_n	Δy_n	Δx_t	Δz_t	Δx_f	Δy_f
f	$\mathbf{m}_1,\mathbf{c}_1$	1	0	0	0	-1	0
e	$\mathbf{m}_2,\mathbf{c}_2$	0	1	0	1	0	-1
c	$\mathbf{C}_3$	0	1	0	0	0	1
a	$\mathbf{m}_4,\mathbf{c}_4$	1	0	1	0	1	0
c	$\mathbf{m}_5,\mathbf{c}_5$	0	1	0	0	0	1
d	$\mathbf{m}_6,\mathbf{c}_6$	0	0	0	1	0	0
e	$\mathbf{m}_7,\mathbf{c}_7$	0	1	0	1	0	-1
d	$\mathbf{m}_8,\mathbf{c}_8$	0	0	0	1	0	0
c	$\mathbf{m}_9,\mathbf{c}_9$	0	1	0	0	0	1
a	$\mathbf{m}_{10},\mathbf{c}_{10}$	1	0	1	0	1	0
d	$\mathbf{m}_{11},\mathbf{c}_{11}$	0	0	0	1	0	0
c	$\mathbf{m}_{12},\mathbf{c}_{12}$	0	1	0	0	0	1
a	$\mathbf{m}_{13},\mathbf{c}_{13}$	1	0	1	0	1	0
a	$\mathbf{m}_{14},\mathbf{c}_{14}$	1	0	1	0	1	0
c	$\mathbf{m}_{15},\mathbf{c}_{15}$	0	1	0	0	0	1
a	$\mathbf{c}_{16}$	1	0	1	0	1	0
b	$\mathbf{c}_{17}$	0	1	0	1	0	1
a	$\mathbf{c}_{18}$	1	0	1	0	1	0
e	$\mathbf{c}_{19}$	0	1	0	1	0	-1

A basis for the null space of $\mathbf{A}^r$, obtained using the MATLAB package, is $(0, -1, 1, 1, 0, 0)'$, hence, $\mathbf{b} = \mathbf{c} + \mathbf{d}$. Resorting to the sparcity of effects principle [14], alternative solutions can be obtained by leaving $\mathbf{b}$, $\mathbf{c}$ and $\mathbf{d}$ out of the basis. Each alternative solution is obtained assuming that one of the patterns does not contribute to machining and camera errors. This will be illustrated in Section VIII.

Finally, the following pairs of basis elements are orthogonal to each other: $\{\mathbf{a}, \mathbf{b}\}$, $\{\mathbf{a}, \mathbf{c}\}$, $\{\mathbf{a}, \mathbf{d}\}$, $\{\mathbf{a}, \mathbf{e}\}$, $\{\mathbf{a}, \mathbf{f}\}$, $\{\mathbf{b}, \mathbf{f}\}$, $\{\mathbf{c}, \mathbf{d}\}$, $\{\mathbf{c}, \mathbf{e}\}$, $\{\mathbf{c}, \mathbf{f}\}$, $\{\mathbf{d}, \mathbf{f}\}$ and $\{\mathbf{e}, \mathbf{f}\}$. Also $\{\mathbf{b}, \mathbf{c}\}$, $\{\mathbf{b}, \mathbf{d}\}$, $\{\mathbf{b}, \mathbf{e}\}$ and $\{\mathbf{d}, \mathbf{e}\}$ are non-orthogonal.

VIII. APPLICATION TO ARTIFACT DATA

The role of artifact studies in the re-certification process has been explained in Section IV.A: an artifact is a particular type of stringer that is pre-drilled and certified on a CMM machine. Certified artifacts are used in re-certification process to measure the error that is due to the vision system. The data that will be analyzed in this section comes from the certification process of an artifact, therefore, the nominal, actual, and camera-recorded coordinates of the holes, which are illustrated in Figure 8, are available.

This study involves analysis of two hole types, namely type A and type B, on a single artifact. There are 28 holes of type A, and 28 holes of type B, which are drilled 0.25 inches apart from each other. That is, the hole number 1 of type A is drilled 0.25 inches apart from hole number 1 of type B on the same surface (near-side, far-side or top), etc. Holes are numbered from 1 to 28 according to the drilling sequence. Hence, the X coordinates of the holes increase as the hole number in each type increases from 1 to 28. The drilling of holes of type A and B are performed independently; first holes of type A are drilled, then the stringer is detached and

repositioned on the drill, and finally holes of type B are drilled. Therefore, the two sets of measurements are independent of each other in every aspect except that they are subject to the shape imperfections of the same stringer (see Section IV.B).

The process-oriented basis elements for the 28 holes of an artifact can be generated by repeating the patterns given in Table I for all the near-side, far-side and top holes. The result is given in Table II. It can been in Table II that there are 14 near-side holes, 7 far-side holes, and 7 top holes, hence, the numbers are not balanced. However, this fact does not change the dependency structure obtained in Section VII ($\mathbf{b} = \mathbf{c} + \mathbf{d}$). In fact, the dependency structure is preserved as long as there are at least one near-side, one far-side, and one top hole on a stringer. Note that while the dependency structure does not change, varying number of holes may change the degree of non-orthogonality between basis elements.

The data sets from holes of type A and B are given in Table III. The data is in the order of one-thousandth of an inch. As explained in Section V, Camera Error and Machining Error are defined as Camera Error = CAMERA - ACTUAL, and Machining Error = ACTUAL - NOMINAL. Therefore, Δx, Δy, and Δz in Table III are equivalent to $x_{Camera} - x_{Actual}$, $y_{Camera} - y_{Actual}$, and $z_{Camera} - z_{Actual}$ for camera errors, and $x_{Actual} - x_{Nominal}$, $y_{Actual} - y_{Nominal}$, and $z_{Actual} - z_{Nominal}$ for machining errors.

We regress the four columns of data in Table III against the process-oriented basis elements in Table II leaving one of the basis elements $\mathbf{b}$, $\mathbf{c}$, or $\mathbf{d}$ out of the basis at a time because of the dependency problem. The POBREP coefficients are presented in Table IV.

It is clear from the discussion in Section IV.A that the problems modeled by POBREP are mechanical or machine-geometry problems, hence, they are expected to remain for many production pieces unless the problem is corrected. Therefore, POBREP should not be used in SPC context, but as a diagnosis tool for the persistent problems of the machine. In this respect, practical significance of POBREP coefficients should be examined instead of statistical significance. Engineering tolerances for most cycle types (types of holes on a stringer) are around three- to four-thousandth of an inch. Using this information, any deviation above one-thousandth of an inch can be considered practically significant as a conservative measure. Note that POBREP coefficients give the degree of deviation patterns modeled by the basis elements in the order of one-thousandth of inch.

Therefore, the practically significant coefficients for machining errors in Table IV are $r_\mathbf{d}$ for $\mathbf{A}^r_\mathbf{m} = [\mathbf{a} \mid \mathbf{c} \mid \mathbf{d} \mid \mathbf{e} \mid \mathbf{f}]$ and $\mathbf{A}^r_\mathbf{m} = [\mathbf{a} \mid \mathbf{b} \mid \mathbf{d} \mid \mathbf{e} \mid \mathbf{f}]$, and $r_\mathbf{b}$ and $r_\mathbf{c}$ for $\mathbf{A}^r_\mathbf{m} = [\mathbf{a} \mid \mathbf{b} \mid \mathbf{c} \mid \mathbf{e} \mid \mathbf{f}]$ for both of the hole types A and B. Similarly, the practically significant coefficients for camera errors of hole type A are $p_\mathbf{d}$ and $p_\mathbf{f}$ for $\mathbf{A}^r_\mathbf{c} = [\mathbf{a} \mid \mathbf{c} \mid \mathbf{d} \mid \mathbf{e} \mid \mathbf{f}]$ and $\mathbf{A}^r_\mathbf{c} = [\mathbf{a} \mid \mathbf{b} \mid \mathbf{d} \mid \mathbf{e} \mid \mathbf{f}]$, and $p_\mathbf{b}$, $p_\mathbf{c}$ and $p_\mathbf{f}$ for $\mathbf{A}^r_\mathbf{c} = [\mathbf{a} \mid \mathbf{b} \mid \mathbf{c} \mid \mathbf{e} \mid \mathbf{f}]$. These coefficients are also significant for the respective bases for hole type B, in addition, $p_\mathbf{e}$ is significant for all the three bases for hole type B.

The dependency between **b**, **c**, and **d** makes it difficult to interpret these results. But in simple terms, if a quality engineer has reasons to believe that the problems linked with one of **a**, **b** or **c** do not affect the system, then the results from the corresponding basis can be used. For instance, if the basis element **d** is not believed to be active, then the significant coefficients r_b and r_c indicate that one or several of the problems linked with the patterns **b** and **c** can be causing a significant machining error. Moreover, the significant coefficients p_b, p_c, p_e and p_f from the analysis of camera errors indicate that the problems linked with the patterns **b**, **c**, **e**, and **f** can be causing a significant camera error. Since the patterns **b** and **c** are detected by both the camera and machining analyses, the engineer may want to start searching the potential problems linked with these two patterns before searching for the patterns **e** and **f**.

Table IV reveals that coefficients for hole type A and B are close to each other. This is another justification of the fact that the problems that are modeled by POBREP are persistent.

IX. CONCLUSION

The application of POBREP to stringer drilling is interesting from a methodological point of view. It presents an opportunity to model metrology errors as well as machining errors in a single POBREP application. POBREP has not been originally developed for metrology problems. Another interesting issue is the statistical monitoring of the POBREP coefficients in this application. Typically it is assumed that POBREP coefficients are i.i.d. normally distributed. In this case, however, a problem persists with almost the same degree for all the stringers that are machined unless a re-calibration occurs on the error source, hence, POBREP coefficients for one problem over multiple stringers will be strongly correlated. This is a common problem for SPC based on POBREP coefficients. The issue of practical versus statistical significance comes into picture at this point: in this application assembly requirements make it clear whether the POBREP coefficients indicate a practically significant error. There are also multivariate techniques for monitoring auto-correlated data, which might be used for statistical monitoring of the POBREP coefficients.

Hole Number	Hole Type	Camera-CMM	a	b	c	d	e	f
6	f	Δx	1	0	0	0	0	-1
		Δy	0	1	1	0	-1	0
7	n	Δx	1	0	0	0	0	1
		Δy	0	1	1	0	1	0
8	t	Δx	1	0	0	0	0	0
		Δz	0	1	0	1	1	0
9	n	Δx	1	0	0	0	0	1
		Δy	0	1	1	0	1	0
10	f	Δx	1	0	0	0	0	-1
		Δy	0	1	1	0	-1	0
11	n	Δx	1	0	0	0	0	1
		Δy	0	1	1	0	1	0
12	t	Δx	1	0	0	0	0	0
		Δz	0	1	0	1	1	0
13	n	Δx	1	0	0	0	0	1
		Δy	0	1	1	0	1	0
14	f	Δx	1	0	0	0	0	-1
		Δy	0	1	1	0	-1	0
15	n	Δx	1	0	0	0	0	1
		Δy	0	1	1	0	1	0
16	t	Δx	1	0	0	0	0	0
		Δz	0	1	0	1	1	0
17	n	Δx	1	0	0	0	0	1
		Δy	0	1	1	0	1	0
18	f	Δx	1	0	0	0	0	-1
		Δy	0	1	1	0	-1	0
19	n	Δx	1	0	0	0	0	1
		Δy	0	1	1	0	1	0
20	t	Δx	1	0	0	0	0	0
		Δz	0	1	0	1	1	0
21	n	Δx	1	0	0	0	0	1
		Δy	0	1	1	0	1	0
22	f	Δx	1	0	0	0	0	-1
		Δy	0	1	1	0	-1	0
23	n	Δx	1	0	0	0	0	1
		Δy	0	1	1	0	1	0
24	t	Δx	1	0	0	0	0	0
		Δz	0	1	0	1	1	0
25	n	Δx	1	0	0	0	0	1
		Δy	0	1	1	0	1	0
26	f	Δx	1	0	0	0	0	-1
		Δy	0	1	1	0	-1	0
27	n	Δx	1	0	0	0	0	1
		Δy	0	1	1	0	1	0
28	t	Δx	1	0	0	0	0	0
		Δz	0	1	0	1	1	0

TABLE III
MACHINING AND CAMERA ERRORS FOR HOLES OF TYPE A AND B

Hole ID	Hole Type	Coordinate	Machining Error		Camera Error	
			Error for Holes A	Error for Holes B	Error for Holes A	Error for Holes B
1	n	Δx	-0.55	1.36	-2.95	0.56
		Δy	-1.22	-0.96	-1.12	-1.46
2	f	Δx	3.37	4.16	3.37	5.46
		Δy	1.82	2.22	2.72	2.72
3	n	Δx	0.36	-0.13	0.66	-0.93
		Δy	0.04	-0.35	0.04	0.05
4	t	Δx	1.92	3.07	0.92	3.67
		Δz	5.29	5.22	5.89	5.62
5	n	Δx	0.69	0.5	-2.21	-0.70
		Δy	-0.39	-0.74	0.01	-0.74
6	f	Δx	0.69	2.78	0.79	3.68
		Δy	-0.39	0.85	-0.09	1.65
7	n	Δx	-0.77	-0.01	-0.37	-0.31
		Δy	-0.29	0.01	-0.79	0.21
8	t	Δx	1.58	2.39	1.48	2.29
		Δz	3.79	4.88	4.19	5.38

TABLE II
PROCESS-ORIENTED BASIS ELEMENTS FOR AN ARTIFACT

Hole Number	Hole Type	Camera -CMM	Process-Oriented Basis Elements					
			a	b	c	d	e	f
1	n	Δx	1	0	0	0	0	1
		Δy	0	1	1	0	1	0
2	f	Δx	1	0	0	0	0	-1
		Δy	0	1	1	0	-1	0
3	n	Δx	1	0	0	0	0	1
		Δy	0	1	1	0	1	0
4	t	Δx	1	0	0	0	0	0
		Δz	0	1	0	1	1	0
5	n	Δx	1	0	0	0	0	1
		Δy	0	1	1	0	1	0

9	n	Δx	-0.59	-0.12	-3.39	-1.62
		Δy	-2.00	-1.8	-2.00	-1.80
10	f	Δx	2.23	2.49	2.13	3.19
		Δy	-0.29	-0.41	0.31	0.49
11	n	Δx	0.61	-0.09	1.41	0.21
		Δy	-0.04	0.01	0.26	0.01
12	t	Δx	1.13	1.55	0.23	1.15
		Δz	4.76	4.17	5.26	4.67
13	n	Δx	-0.62	-0.27	-2.82	-1.47
		Δy	-0.67	-0.88	-0.07	-0.68
14	f	Δx	1.62	1.57	1.52	2.47
		Δy	0.16	0.63	0.76	1.33
15	n	Δx	0.35	-0.28	0.55	-0.88
		Δy	0.20	0.09	-0.60	-0.11
16	t	Δx	1.05	1.23	0.05	1.53
		Δz	3.11	2.73	3.41	3.13
17	n	Δx	-0.95	-0.52	-3.75	-1.62
		Δy	-0.69	-1.67	-0.69	-1.37
18	f	Δx	1.51	1.12	1.61	1.72
		Δy	1.26	2.27	1.76	2.87
19	n	Δx	0.48	-0.16	0.78	-0.26
		Δy	0.19	0.36	0.89	0.36
20	t	Δx	0.53	0.52	-0.17	0.32
		Δz	3.02	0	3.32	0.30
21	n	Δx	-0.31	-0.36	-3.01	-1.06
		Δy	-0.07	-1.43	0.43	-1.63
22	f	Δx	0.45	0.33	0.65	0.83
		Δy	2.19	3.09	3.29	3.79
23	n	Δx	0.01	0.13	0.21	-0.17
		Δy	-0.05	-0.24	0.05	0.26
24	t	Δx	-0.09	0.48	-1.59	0.28
		Δz	2.96	1.59	4.06	2.09
25	n	Δx	-0.91	-0.8	-3.51	-2.80
		Δy	-1.40	4.25	-1.30	4.35
26	f	Δx	-0.08	-0.5	-0.08	0.30
		Δy	-0.18	0.5	0.52	1.20
27	n	Δx	-0.03	0.32	0.27	1.02
		Δy	0.03	0.23	0.43	1.23
28	t	Δx	-3.53	-7.15	-3.43	-8.05
		Δz	1.32	-0.54	1.42	-0.24

An important drawback of POBREP for this application is that many basis elements are linearly dependent. Despite the high dimensional error vector from a stringer the maximum number of linearly dependent basis elements is 6. This situation considerably restricts precise diagnosis from several potential problems that might be affecting the system. On the other hand, detection of a problem via POBREP can eliminate 5 out of 6 classes of possible causes.

POBREP analysis for both camera and machining errors requires the actual coordinates of the holes, which can be measured by a high precision CMM machine. A possible strategy to eliminate the need for a CMM study and to diagnose problems directly from reported errors would be to develop POBREP basis elements for reported errors. However, such basis elements exist only for a small set of problems examined in this study. That is, many of the problems do not induce an error pattern on the reported errors. The ones that induce an error pattern, on the other hand, can still be modeled by POBREP, but the diagnostic information would be very limited in this case. Note that the patterns observed in Section IV.A (Figures 6 and 7) are the results of such problems.

TABLE IV
POBREP COEFFICIENTS FOR MACHINING AND CAMERA ERRORS

Error Type	Basis	POBREP Coefficients
Machine for A	[a|c|d|e|f]	$(r_\mathbf{a}, r_\mathbf{c}, r_\mathbf{d}, r_\mathbf{e}, r_\mathbf{f})$= (0.552, 0.099, 4.018, -0.554, -0.756)
Machine for A	[a|b|d|e|f]	$(r_\mathbf{a}, r_\mathbf{b}, r_\mathbf{d}, r_\mathbf{e}, r_\mathbf{f})$= (0.552, 0.099, 3.919, -0.554, -0.756)
Machine for A	[a|b|c|e|f]	$(r_\mathbf{a}, r_\mathbf{b}, r_\mathbf{c}, r_\mathbf{e}, r_\mathbf{f})$= (0.552, 4.018, -3.919, -0.554, -0.756)
Machine for B	[a|c|d|e|f]	$(r_\mathbf{a}, r_\mathbf{c}, r_\mathbf{d}, r_\mathbf{e}, r_\mathbf{f})$= (0.691, 0.542, 3.344, -0.765, -0.820)
Machine for B	[a|b|d|e|f]	$(r_\mathbf{a}, r_\mathbf{b}, r_\mathbf{d}, r_\mathbf{e}, r_\mathbf{f})$= (0.691, 0.542, 2.801, -0.765, -0.820)
Machine for B	[a|b|c|e|f]	$(r_\mathbf{a}, r_\mathbf{b}, r_\mathbf{c}, r_\mathbf{e}, r_\mathbf{f})$= (0.691, 3.344, -2.801, -0.765, -0.820)
Camera for A	[a|c|d|e|f]	$(p_\mathbf{a}, p_\mathbf{c}, p_\mathbf{d}, p_\mathbf{e}, p_\mathbf{f})$= (-0.050, 0.503, 4.757, -0.821, -1.323)
Camera for A	[a|b|d|e|f]	$(p_\mathbf{a}, p_\mathbf{b}, p_\mathbf{d}, p_\mathbf{e}, p_\mathbf{f})$= (-0.050, 0.503, 4.254, -0.821, -1.323)
Camera for A	[a|b|c|e|f]	$(p_\mathbf{a}, p_\mathbf{b}, p_\mathbf{c}, p_\mathbf{e}, p_\mathbf{f})$= (-0.050, 4.757, -4.254, -0.821, -1.323)
Camera for B	[a|c|d|e|f]	$(p_\mathbf{a}, p_\mathbf{c}, p_\mathbf{d}, p_\mathbf{e}, p_\mathbf{f})$= (0.703, 0.956, 4.044, -1.051, -1.552)
Camera for B	[a|b|d|e|f]	$(p_\mathbf{a}, p_\mathbf{b}, p_\mathbf{d}, p_\mathbf{e}, p_\mathbf{f})$= (0.703, 0.956, 3.087, -1.051, -1.552)
Camera for B	[a|b|c|e|f]	$(p_\mathbf{a}, p_\mathbf{b}, p_\mathbf{c}, p_\mathbf{e}, p_\mathbf{f})$= (0.703, 4.044, -3.087, -1.051, -1.552)

X.   REFERENCES

[1]   R. R. Barton and D. R. González-Barreto, "Process Oriented Basis Representations for Multivariate Process Diagnostics", *Quality Engineering*, Vol. 9, pp. 107-118, 1996.
[2]   B. Birgoren, *Multivariate Statistical Process Control for Quality Diagnostics and Applications to Process Oriented Basis Representations*, Ph.D. Thesis, PennState University, Pennsylvania, 1998.
[3]   B. Birgören, "A Method for Problem Diagnosis in Multivariate Quality Control: Constrained Solution Spaces for Process Oriented Basis Representations", *Teknoloji*, Vol. 7 No. 1, pp. 19-28, 2004.
[4]   H. I. Espada Colon and D. R. Gonzalez-Barreto, "Component Registration Diagnosis for Printed Circuit Boards using Process-Oriented Basis Elements", *Computers & Industrial Engineering*, Vol. 33, pp. 389-392, 1997.
[5]   E. J. Foster, R. R. Barton, N. Gautam, L. T. Truss and J. D. Tew, "The Process-oriented Multivariate Capability Index", *International Journal of Production Research*, Vol. 43, No. 10, pp. 2135-2148, 2005.
[6]   G. C. Runger, R. R. Barton, E. D. Castillo and W. H. Woodall, "Optimal Monitoring of Multivariate Data for Fault Patterns", *Journal of Quality Technology*, Vol. 39, No. 2, pp. 159-172, 2007.
[7]   C. A. Lowry and D. C. Montgomery, "A Review of Multivariate Control Charts", *IIE Transactions*, Vol. 27, pp. 800-810, 1995.
[8]   D. W. Apley and J. Shi, "A Factor-Analysis Method for Diagnosing Variability in Multivariate Manufacturing Processes", *Technometrics*, Vol. 43, pp 84-95, 2001.
[9]   H. Y. Lee and D. W. Apley, "Diagnosing Manufacturing Variation Using Second-Order and Fourth-Order Statistics", *International Journal of Flexible Manufacturing Systems*, Vol. 16, pp 45-64, 2004.
[10] R. L. Mason, J. C. Young, *Multivariate Statistical Process Control with Industrial Application*, ASA-SIAM, Philadelphia, PA, 2001.
[11] Y. Ding, L. Zheng and S. Zhou, "Phase-I Analysis for Monitoring Nonlinear Profile Signals in Manufacturing Processes", *Journal of Quality Technology*, Vol. 38, pp 199-216, 2006.
[12] D. W. Apley and H. Y. Lee, "Identifying Spatial Variation Patterns in Multivariate Manufacturing Processes: A Blind Search Approach", *Technometrics*, Vol. 45, pp 220-234, 2003.
[13] N. Jin and S. Zhou, "Data-Driven Variation Source Identification of Manufacturing Processes Based on Eigenspace Comparison", *Naval Search Logistics*, Vol. 53, pp. 383-396, 2006.
[14] J. Neter, M. H. Kutner, C. J. Nachtsheim and W. Wasserman, *Applied Linear Statistical Models* (4th edition), McGraw-Hill/Irwin, IL, 1996.